5042 *Chem. Mater.* **2009,** *21,* 5042–5049
DOI:10.1021/cm901109n

CHEMISTRY OF MATERIALS
Article

Void Space Containing Crystalline Cu(I) Phenanthroline Complexes As Molecular Oxygen Sensors

Conor S. Smith and Kent R. Mann*

Department of Chemistry, University of Minnesota, Minneapolis, Minnesota 55455

Received April 22, 2009. Revised Manuscript Received August 12, 2009

We have shown that crystals of a number of emissive copper compounds of the form $[Cu(NN)_2]X$ (X = BF_4^-, $tfpb^-$) (where NN = 1,10-phenanthroline (phen), 2,9-dimethyl-1,10-phenanthroline (dmp), 2,9-dimethyl-4,7-diphenyl-1,10-phenanthroline (bdmp), 2,9-diisopropyl-1,10-phenanthroline (dipp), 2,9-di-tert-butyl-1,10-phenanthroline (dbp); $tfpb^-$ = tetrakis(bis-3,5-trifluoromethylphenylborate) are oxygen sensors, if they contain void space. All of the $tfpb^-$ salts were found to be oxygen sensors reinforcing the idea that bulky counterions can produce void space and obviate the need for a support material in solid-state photoluminescent oxygen sensors. The reponse time for the X = $tfpb^-$ and NN = dipp complex was measured to be fast (280 ms (95% of final value)). The first solid-state quantum yields and lifetimes are reported for the $[Cu(NN)_2]X$ systems and are found to be approximately 10 times larger than those observed in solution-state measurements. The linear Stern−Volmer plots with highly reproducible K_{sv} constants observed from sample to sample and day to day reinforce the observations that the sensing materials are crystalline, stable to air and light, and the sensing sites are homogeneous within the crystals.

Introduction

Transition metal complexes have long been used as oxygen sensors in solution or when dispersed in polymer films or sol gels.[1−4] The disadvantages of these systems include nonuniformity of emitting sites,[5] slow response times,[6,7] and photochemical degradation of either the lumiphor or the support matrix by the reactive oxygen species produced by the quenching events.[8] Additionally, most of the previously reported photoluminescent oxygen sensors utilize expensive transition metals in the active material.[2] Our recent work with crystalline oxygen sensors[9−11] demonstrated that support media are not necessary for photoluminescent oxygen sensors and these crystalline materials offer certain advantages in stability and uniformity of emission sites. Recently, we have set out to synthesize and study oxygen sensors that use a crystalline, inexpensive, first row transition metal complex as the active sensing material to decrease their price and maximize the crystalline solid advantages. Crystalline systems based on Cu(I) derivatives that have been reported to sense oxygen in polymer supports[12,13] seemed excellent candidates for the active material but are also problematic in several ways.

For example, the extensive studies of [Cu(phenanthroline-derivative)$_2$]$^+$ ($[Cu(NN)_2]^+$) systems by McMillin[14−18] and others[19,20] have shown them to be very weakly emissive in solution unless sufficient steric restriction in the 2- and 9-positions of the phenanthroline ligands is present. These steric restrictions minimize the distortion that occurs when the molecule is excited and decrease the nonradiative pathways that quench the emission from the MLCT excited state.[21]

*Corresponding author. E-mail: krmann@umn.edu.

(1) Leventis, N.; Elder, I. A.; Rolison, D. R.; Anderson, M. L.; Merzbacher, C. I. *Chem. Mater.* **1999**, *11*, 2837–2845.
(2) Demas, J. N.; DeGraff, B. A.; Coleman, P. B. *Anal. Chem.* **1999**, *71*, 793A–800A.
(3) Krenske, D.; Abdo, S.; Van Damme, H.; Cruz, M.; Fripiat, J. J. *J. Phys. Chem.* **1980**, *84*, 2447–57.
(4) Lin, C.-T.; Sutin, N. *J. Phys. Chem.* **1976**, *80*, 97–105.
(5) Demas, J. N.; DeGraff, B. A.; Xu, W. *Anal. Chem.* **1995**, *67*, 1377–80.
(6) Bowyer, W. J.; Xu, W.; Demas, J. N. *Anal. Chem.* **2004**, *76*, 4374–4378.
(7) Kneas, K. A.; Demas, J. N.; Nguyen, B.; Lockhart, A.; Xu, W.; DeGraff, B. A. *Anal. Chem.* **2002**, *74*, 1111–1118.
(8) Carraway, E. R.; Demas, J. N.; DeGraff, B. A.; Bacon, J. R. *Anal. Chem.* **1991**, *63*, 337–42.
(9) McGee, K. A.; Mann, K. R. *J. Am. Chem. Soc.* **2009**, *131*, 1896–1902.
(10) McGee, K. A.; Marquardt, B. J.; Mann, K. R. *Inorg. Chem.* **2008**, *47*, 9143–9145.
(11) McGee, K. A.; Veltkamp, D. J.; Marquardt, B. J.; Mann, K. R. *J. Am. Chem. Soc.* **2007**, *129*, 15092–15093.
(12) Miller, M. T.; Karpishin, T. B. *Sens. Actuators, B* **1999**, *B61*, 222–224.
(13) Shi, L.; Li, B.; Yue, S.; Fan, D. *Sens. Actuators, B* **2009**, *B137*, 386–392.
(14) Everly, R. M.; Ziessel, R.; Suffert, J.; McMillin, D. R. *Inorg. Chem.* **1991**, *30*, 559–61.
(15) Palmer, C. E. A.; McMillin, D. R. *Inorg. Chem.* **1987**, *26*, 3837–40.
(16) Ichinaga, A. K.; Kirchhoff, J. R.; McMillin, D. R.; Dietrich-Buchecker, C. O.; Marnot, P. A.; Sauvage, J. P. *Inorg. Chem.* **1987**, *26*, 4290–2.
(17) McMillin, D. R.; Gamache, R. E. Jr.; Kirchhoff, J. R.; Del Paggio, A. A. *Copper Coord. Chem.: Biochem. Inorg. Perspect.* **1983**, 223–35.
(18) Rader, R. A.; McMillin, D. R.; Buckner, M. T.; Matthews, T. G.; Casadonte, D. J.; Lengel, R. K.; Whittaker, S. B.; Darmon, L. M.; Lytle, F. E. *J. Am. Chem. Soc.* **1981**, *103*, 5906–12.
(19) Miller, M. T.; Gantzel, P. K.; Karpishin, T. B. *Inorg. Chem.* **1999**, *38*, 3414–3422.
(20) Miller, M. T.; Karpishin, T. B. *Inorg. Chem.* **1999**, *38*, 5246–5249.
(21) Cunningham, C. T.; Moore, J. J.; Cunningham, K. L. H.; Fanwick, P. E.; McMillin, D. R. *Inorg. Chem.* **2000**, *39*, 3638–3644.

Published on Web 10/07/2009

Even so, these restricted complexes have relatively short lifetimes (hundreds of nanoseconds)[22] and low quantum yields (~0.002) in solution but have been shown to have more favorable lifetimes and quantum yields in rigid media like polymers[12] and low-temperature glasses.[14] Our goal is to produce crystalline Cu(I)-based oxygen sensors that replace the slow but solution like diffusion provided by typical polymer supports[6,7] with a suitably designed crystal lattice with void space that is sufficient to allow diffusional oxygen quenching of the excited state. This type of crystalline material also offers the possibility of reproducibility between sensors, i.e., each sample of the pure solid will have the same sensing ability. With this goal in mind, a number of $[Cu(NN)_2]X$ ($X^- = BF_4^-$, $tfpb^-$; where $tfpb^-$ = tetrakis(bis-3,5-trifluoromethylphenylborate)) compounds were synthesized and examined for oxygen sensing and photophysical properties. We have found that all of the crystalline $tfpb^-$ salts (and in one case, a BF_4^- salt) of $[Cu(NN)_2]^+$ can be used as molecular oxygen sensors. We have also obtained solid state photophysical data for these compounds that show they have high solid-state quantum yields and longer emission lifetimes relative to solution measurements. The complexes reported here are not as sensitive as the $Ru(NN)_3^{2+}$ or Pt porphorin systems that are currently in use but rather are prototypes that warrant further development via synthetic elaboration (in progress).

Experimental Section

General Considerations. $Cu(BF_4)_2 \cdot XH_2O$ was purchased from Aldrich Chemical Co. and used as received. The solvents (dichloromethane, methanol, diethyl ether, acetonitrile, hexanes, and toluene) were obtained from commercial sources and either used without further purification or after drying with molecular sieves. The ligands 1,10-phenanthroline (phen), 2,9-dimethyl-1,10-phenanthroline (dmp), and 2,9-dimethyl-4,7-diphenyl-1,10-phenanthroline (bdmp) were purchased from Aldrich. 2,9-Diisopropyl-1,10-phenanthroline (dipp) and 2,9-ditert-butyl-1,10-phenanthroline (dbp) were synthesized by a literature procedure.[23] Sodium(tetrakis(bis-3,5-trifluoromethyl(phenylborate))) (Natfpb) was available from a previous study.[24] $[Cu(CH_3CN)_4]BF_4$ was synthesized by a literature procedure.[25]

A 300 MHz Varian Unity NMR spectrometer was utilized to obtain the ^1H and ^{19}F NMR spectra. Chemical shifts are reported in units of ppm with an external reference to the residual proton resonance in deuterated dichloromethane or chloroform for ^1H NMR spectra and the internal $CFCl_3$ reference for the ^{19}F NMR. High-resolution mass spectrometry was carried out on a Bruker BioTOF II mass spectrometer.

Synthesis and Characterization. The $[Cu(NN)_2]BF_4$ complexes used in this study were synthesized as previously reported[21] by adding the substituted phen ligand to a solution of $[Cu(CH_3CN)_4]BF_4$ in CH_2Cl_2 followed by precipitation of the salt with diethyl ether. The metatheses to the $tfpb^-$ salts were carried out by adding a 1.2:1 ratio of Natfpb to $[Cu(NN)_2]BF_4$ in MeOH. Precipitation with water yielded pure compounds. The complete conversion by this metathesis route was confirmed by the presence of signals for $tfpb^-$ and the absence of signals for BF_4^- in the ^{19}F NMR of the products. The syntheses of $[Cu(dmp)_2]BF_4$ (**1a**), $[Cu(bdmp)_2]BF_4$ (**2a**), $[Cu(dipp)_2]tfpb$ (**3b**), and $[Cu(dmp)(dbp)BF_4$ (**4a**) have previously been reported elsewhere.[16,21,26,27] NMR and mass spectrometry confirmed the purity of these compounds. The synthesis and characterization of $[Cu(dmp)_2]tfpb$ (**1b**), $[Cu(bdmp)_2]tfpb$ (**2b**), $[Cu(dipp)_2]BF_4$ (**3a**), and [Cu(dmp)(dbp)]tfpb (**4b**) are given below.

[Cu(dmp)$_2$]tfpb (1b). $[Cu(dmp)_2]BF_4$ (0.0300 g, 0.051 mmol) was dissolved in 20 mL of MeOH. Natfpb (0.0456 g, 0.052 mmol) was added and then the addition of water yielded a bright orange precipitate. After filtration, the orange solid was dried under a vacuum to yield 0.0394 g (57% yield) of product. X-ray quality crystals were grown from methanol/water. ^{1}NMR (CD_2Cl_2) δ 8.455 (d, 4 H, J = 8.4 Hz), 8.004 (s, 4 H), 7.73, (d, 4 H, J = 8.4 Hz), 7.716 (br s, 8 H), 7.545 (br s, 4 H), 2.415 (s, 12 H). ^{19}F NMR (CD_2Cl_2) δ −63.540 (s, 24 F). HRESIMS (M^+): calcd for $C_{28}H_{24}CuN_4$, 479.1291; found, 479.1285.

[Cu(bdmp)$_2$]tfpb (2b). Natfpb (0.0986 g, 0.10 mmol) was added to 50 mL of MeOH. This solution was added to a $[Cu(bdmp)_2]BF_4$ (0.0761 g, 0.080 mmol) solution in 70 mL of MeOH and stirred for 10 min. The solution was then evaporated to dryness, redissolved in MeOH, precipitated with water, and filtered to yield 0.126 g (95% yield) of product. ^{1}NMR (CD_2Cl_2) δ 8.071 (d, 4 H, J = 3.3 Hz), 7.718 (s, 4 H), 7.689 (d, 4 H, J = 7.2 Hz), 7.677 (br s, 8 H), 7.593 (br s, 20 H), 7.464 (br s, 4 H), 2.548 (s, 12 H) ^{19}F NMR (CD_2Cl_2) δ −63.131 (s, 24 F). HRESIMS (M^+): calcd for $C_{52}H_{40}CuN_4$, 783.2543; found, 783.2571.

[Cu(dipp)$_2$]BF$_4$ (3a). $[Cu(NCCH_3)_4]BF_4$ (0.142 g, 0.470 mmol) was dissolved in 50 mL of acetonitrile. Addition of dipp (0.262 g, 0.945 mmol) gave a dark red clear solution that was evaporated to dryness, redissolved in methanol, and precipitated with water to yield a bright red product after filtration. Drying the bright red solid under a vacuum yielded 0.249 g (78% yield) of product. ^{1}NMR (CD_2Cl_2) δ 8.632 (d, 4 H, 8.4 Hz), 8.112 (s, 4 H), 7.816 (d, 4 H, J = 8.7 Hz), 0.985 (s, 24 H) ^{19}F NMR (CD_2Cl_2) δ −154.669 (s, 4 F). HRESIMS (M^+): calcd for $C_{36}H_{40}CuN_4$, 591.2543; found, 591.2579.

[Cu(dmp)(dbp)]tfpb (4b). $[Cu(dbp)(dmp)]BF_4$ (0.0313 g, 0.0481 mmol) was dissolved in 70 mL of MeOH. Natfpb (0.0526 g, 0.0560 mmol) was added and the orange solution was stirred for 5 min. Water was added to precipitate the product, which was filtered producing 0.0882 g of a mixture of $[Cu(dmp)_2]tfpb$ and [Cu(dmp)(dbp)]tfpb. The recrystallization from MeOH/water yielded both small dark and large light-red crystals. Under UV lamp illumination, the emission from the large light-red crystals gave significantly brighter emission than the small dark-red crystals. The large (approximately 3 mm per side) light-red blocklike crystals (0.0472 g, 69% yield) were separated by hand and confirmed to be pure heteroleptic [Cu(dmp)(dbp)]tfpb (**4b**) by NMR and X-ray crystallography. The small dark crystals that remained were confirmed to be $[Cu(dmp)_2]tfpb$ (**1b**) by NMR. Data reported for [Cu(dmp)(dbp)]tfpb (**4b**): ^{1}NMR (CD_2Cl_2) δ 8.526 (d, 2 H, J = 8.40 Hz), 8.449 (d, 2H, J = 8.10 Hz), 8.084 (d, 2 H, J = 8.4 Hz), 8.015 (s, 2 H),

(22) Lavie-Cambot, A.; Cantuel, M.; Leydet, Y.; Jonusauskas, G.; Bassani, D. M.; McClenaghan, N. D. *Coord. Chem. Rev.* **2008**, *252*, 2572–2584.
(23) Dietrich-Buchecker, C. O.; Marnot, P. A.; Sauvage, J. P. *Tetrahedron Lett.* **1982**, *23*, 5291–4.
(24) Exstrom, C. L.; Britton, D.; Mann, K. R.; Hill, M. G.; Miskowski, V. M.; Schaefer, W. P.; Gray, H. B.; Lamanna, W. M. *Inorg. Chem.* **1996**, *35*, 549–50.
(25) Dietrich-Buchecker, C.; Sauvage, J. P.; Kern, J. M. *J. Am. Chem. Soc.* **1989**, *111*, 7791–800.
(26) Gandhi, B. A.; Green, O.; Burstyn, J. N. *Inorg. Chem.* (*Washington, DC, U. S.*) **2007**, *46*, 3816–3825.
(27) Klemens, F. K.; Fanwick, P. E.; Bibler, J. K.; McMillin, D. R. *Inorg. Chem.* **1989**, *28*, 3076–9.

Table 1. Crystallographic Data and Refinement Parameters

	1a[a]	1b	2b	3a	4b
empirical formula	$C_{28}H_{24}CuN_4BF_4$	$C_{60}H_{36}CuN_4BF_{24}$	$C_{84}H_{52}CuN_4BF_{24}$	$C_{39}H_{40}CuN_4BF_4$	$C_{66}H_{48}CuN_4BF_{24}$
cryst color, morphology	orange, plate	red, block	yellow, plate	orange, plate	yellow, block
cryst syst	monoclinic	triclinic	triclinic	monoclinic	triclinic
space group	$P2_1/c$	$P\bar{1}$	$P\bar{1}$	$P2_1/c$	$P\bar{1}$
a (Å)	12.514(3)	13.5298(10)	16.171(1)	14.5860(17)	12.9582(9)
b (Å)	18.018(4)	14.5589(10)	16.194(1)	17.2051(19)	13.1246(9)
c (Å)	23.063(5)	16.8576(12)	16.754(1)	14.3183(16)	20.0338(14)
α (deg)	90	104.8500(10)	113.524(1)	90	106.4860(10)
β (deg)	90.103(4)	106.3540(12)	90.951(2)	103.637(2)	100.5770(10)
γ (deg)	90	97.8500(10)	107.560(1)	90	98.1470(10)
V (Å^3)	5200(2)	3000.8(4)	3788(9)	3491.9(7)	3143.0(4)
Z	8	2	2	4	2
formula weight (g mol^{-1})	566.86	1343.28	1647.65	679.07	1427.43
density (calcd) (g cm^{-3})	1.448	1.487	1.445	1.292	1.508
T (K)	173(2)	173(2)	123(2)	173(2)	123(2)
absorption coeff (mm^{-1})	0.893	0.481	0.396	0.677	0.464
F(000)	2320	1348	1668	1416	1444
θ range (deg)	2.17−22.56	1.32−25.06	1.46−27.50	1.86−25.06	1.09−25.05
index ranges	$-14 \le h \le 14$; $0 \le k \le 21$; $0 \le l \le 27$	$-16 \le h \le 16$; $-17 \le k \le 16$; $-18 \le l \le 20$	$-20 \le h \le 20$; $-20 \le k \le 19$; $0 \le l \le 21$	$-17 \le h \le 17$; $-20 \le k \le 20$; $-17 \le l \le 16$	$-15 \le h \le 15$; $-15 \le k \le 14$; $0 \le l \le 23$
no. of reflns collected	9418	22484	17051	18820	11118
no. of independent reflns	9115	10515	17051	6168	11118
weighting factors[b] a, b	0.0487, 7.5760	0.0564, 1.2789	0.0791, 7.1010	0.0828, 2.568	0.0575, 4.2177
max, min transmission	0.9160, 0.6636	0.845, 0.753	0.9503, 0.8419	0.967, 0.638	0.870000, 0.782517
data/restraints/params	9115/0/694	10515/30/877	17051/0/1051	6168/220/504	11118/138/922
R_1, wR_2 [$I > 2\sigma(I)$]	0.0529, 0.1178	0.0543, 0.1220	0.0658, 0.1605	0.0546, 0.1407	0.0465, 0.1147
R_1, wR_2 (all data)	0.0806, 0.1325	0.0875, 0.1334	0.1116, 0.1913	0.1126, 0.1758	0.0653, 0.1287
GOF	1.050	1.031	1.029	1.019	1.023
largest diff. peak, hole (e Å^{-3})	0.620, −0.504	0.370, −0.1344	1.888, −0.809	0.550, −0.221	0.780, −0.477

[a] This compound is a methanol solvate; the methanol was severely disordered and was "squeezed" from the refinement. Details are given in the Supporting Information. [b] $w = [\sigma^2(F_o^2) + (aP)^2 + (bP)]^{-1}$, where $P = (F_o^2 + 2F_c^2)/3$.

8.001 (s, 2 H), 7.723 (br s, 8 H), 7.709 (d, 2H, J = 8.4 Hz), 7.550 (br s, 4 H), 2.437 (s, 6 H), 1.180 (s, 18 H) ^{19}F NMR (CD_2Cl_2) δ −63.525 (s, 24 F). HRESIMS (M^+): calcd for $C_{34}H_{36}CuN_4$, 563.2231; found, 563.2243.

Single-Crystal X-ray Crystallography. The crystal structures of five compounds **1a**, **1b**, **2b**, **3a**, and **4b** were determined in this study. Relevant crystallographic data are shown in Table 1 and details of the structure determinations are given in the Supporting Information. All the data for these structure determinations were collected at the X-ray Crystallographic Laboratory (Department of Chemistry, University of Minnesota). Single crystals were attached to glass fibers and mounted on a Bruker SMART Platform CCD (tfpb$^-$ structures) or Siemens SMART Platform CCD (BF_4^- structures) for data collection at 123 K (tfpb$^-$ structures) or 173 K (BF_4^- structures) using graphite-monochromated Mo Kα radiation (λ = 0.71073 Å). An initial set of cell constants was calculated from reflections harvested from three sets of 20 frames oriented such that orthogonal wedges of reciprocal space were surveyed. Final cell constants were calculated from at least 2860 strong reflections from the actual data collection. Data were collected to the extent of (1.5−2.0) hemispheres at a resolution of 0.84 Å using φ-scans. For all structures, the intensity data were corrected for absorption and decay using SADABS.[28] Solution and refinement were performed utilizing SHELXTL-V6.12.[29] The void space fraction was calculated for these structures and several available in the literature using PLATON/VOID.[30,31] Details for these calculations are given in the Supporting Information.

Although a number of crystal structures are available for the same $[Cu(NN)_2]^+$ systems,[32−34] many of those compounds differed from those in this study by counterion or solvent of crystallization. Because sensing ability depends on the exact anion and the possible existence of polymorphs or solvates, we have found that careful attention to the details of "where did the crystals originally come from and where have they been" is necessary. Therefore, single crystals of 5 of the compounds reported herein, **1a**, **1b**, **2b**, **3a**, and **4b** for X-ray studies were grown exclusively from MeOH/water, and all of the data in Table 2 were obtained with samples that were prepared from methanol. Crystal structure data are available for **2a** and **3b** from previous works[21,27] and were downloaded from the CCDC database.[35] As the crystals for these structures were grown from methanol and ethanol, respectively, we confirmed that the unit

(28) Blessing, R. H. *Acta Crystallogr., Sect. A* **1995**, *A1*, 33–8.
(29) *SHELXTL*, 6.12 ed.; Bruker AXS: Madison, WI, 2001.
(30) Spek, A. L. *J. Appl. Crystallogr.* **2003**, *36*, 7–13.
(31) Spek, A. L. *PLATON/VOID*; Utrecht University: Utrecht, The Netherlands, 2005.
(32) Hoffmann, S. K.; Corvan, P. J.; Singh, P.; Sethulekshmi, C. N.; Metzger, R. M.; Hatfield, W. E. *J. Am. Chem. Soc.* **1983**, *105*, 4608–17.
(33) Cheng, J.-K.; Yin, P.-X.; Li, Z.-J.; Qin, Y.-Y.; Yao, Y.-G. *Inorg. Chem. Commun.* **2007**, *10*, 808–810.
(34) King, G.; Gembicky, M.; Coppens, P. *Acta Crystallogr., Sect. C* **2005**, *61*, m329–m332.
(35) Allen Frank, H. *Acta Crystallogr., Sect. B* **2002**, *58*, 380–8.

Table 2. Summary of Crystallographic, Photophysical, and Oxygen Sensing Data

compds	K_{SV}[a]	λ_{max} (nm)[b]	Φ (N_2)[c]	τ_0 (μs, N_2)[d]	τ (μs, O_2)[e]	% void space[f]	$k_r(10^4)$[g]	$k_{nr}(10^6)$[h]
$[Cu(dmp)_2]BF_4$ (**1a**)[i]	$< 5 \times 10^{-3}$	700	0.009(2)	0.803	0.800	2.1[j]	1	10
$[Cu(dmp)_2]$tfpb·CH_3OH (**1b**)[i]	0.060(1)	700	0.0060(2)	0.664	0.654	0.5	0.90	15
$[Cu(bdmp)_2]BF_4$·CH_3OH (**2a**)[k]	$< 5 \times 10^{-3}$	738	0.0011(5)	0.251	0.243	0	0.44	40
$[Cu(bdmp)_2]$tfpb (**2b**)[i]	0.137(2)	746	0.0039(3)	0.294	0.273	2.8	1.3	34
$[Cu(dipp)_2]BF_4$ (**3a**)[i]	0.103(4)	670	0.050(1)	2.744	2.485	6.3	1.9	3.5
				1.478	1.257			
$[Cu(dipp)_2]$tfpb (**3b**)[l]	0.299(7)	679	0.019(1)	1.170	0.946	3.3	1.7	8.4
$[Cu(dmp)(dbp)]BF_4$ (**4a**)[m]	$< 5 \times 10^{-3}$	602	0.139(1)	5.282	5.266	[m]	2.6	1.6
				1.386	1.381			
[Cu(dmp)(dbp)]tfpb (**4b**)[i]	0.155(4)	608	0.122(1)	3.440	3.069	3.9	3.5	2.6

[a] Estimated limit of detection is 5×10^{-3}. [b] Corrected solid-state emission peak wavelength. [c] Solid-state emission quantum yield under nitrogen. [d] Solid-state emission lifetime under nitrogen. [e] Solid-state emission lifetime under oxygen. [f] Calculated percentage of void space from X-ray crystal structure. [g] Calculated radiative rate constant (s^{-1}). [h] Calculated nonradiative rate constant (s^{-1}). [i] Structure determined here. [j] Void space is isolated pockets. [k] CCDC structure JARBIN.[27] [l] CCDC structure XAFBEL.[21] [m] Structure not determined.

cells of crystals from our sensing samples of **2a** and **3b** (grown from methanol) match the literature values.

O_2 Sensing Apparatus and Procedure. The crystalline films used for gas sensing were prepared by placing small (~1 mg) amounts of crystalline solid on a the end of a 1/4" diameter Delrin rod, followed by addition of a small drop of MeOH to partially dissolve the sample. Slow evaporation of the MeOH resulted in an adherent crystalline film. The heteroleptic compounds **4a** and **4b** slowly isomerize in MeOH solutions, so for these two compounds, single crystals were placed into a depression in a Delrin rod and the solids were not redissolved. Additionally, a single crystal of compound **3b** was tested for oxygen sensing to confirm that the films used for oxygen sensing experiments and the single crystals used for X-ray diffraction gave similar results. In all of these cases, the prepared samples were then placed into the apparatus based on a 1/4 in. diameter swage cross-tube fitting, which is shown schematically in the Supporting Information. A 400 nm LED source filtered through an interference filter is used for excitation through the center fiber of a "six around one" bifurcated fiber optic probe. The emission was collected through the six fiber channel and sent into an Ocean Optics USB-2000 spectrometer. The spectrometer, mass flow controllers, temperature, and pressure monitors were interfaced to a computer to allow control of the unattended data acquisition via a custom Labview program.

The emission data collected were analyzed with a spreadsheet written in Microsoft Excel. Data from three cycles of spectra obtained at approximately 0.0, 0.10, 0.21, 0.25, 0.40, 0.50, 0.65, 0.80, 0.90, and 1.0 mol fraction of O_2 in N_2 were used for the Stern−Volmer plots. The oxygen concentrations for the Stern−Volmer plots reported here are expressed in terms of mole fraction at the standard atmospheric pressure (corrected for elevation) of Minneapolis-St. Paul, MN of 0.97 atm. The acquisitions were at room temperature, approximately 21.8 ± 1 °C. Exact gas mole fractions were calculated by referencing the feedback voltage of the mass flow controllers to a calibration previously performed. The emission intensity was integrated across the entire peak and divided by the integrated LED intensity for each spectrum to give I_0 (intensity under nitrogen) and I (intensity at a given O_2 mixture). $I_0/I - 1$ was plotted vs oxygen mole fraction in nitrogen to yield a Stern−Volmer plot; a linear regression model was used to calculate the slope. The Stern−Volmer slopes from multiple runs taken on separately prepared samples were averaged and the standard deviation was calculated.

Pressure Jump Experiment. A crystalline sample of compound **3b** was deposited from a methanol solution on a brass rod which was placed in a pressure tight version of the swage cross cell complete with the fiber optic probe. The cell was pressurized with air (typically 47.8 psi) and after a suitable equilibration time (a few seconds) an electronic valve was actuated to release the pressure to atmospheric pressure (14.3 psi) in approximately 2 msec. Emission data were obtained for the pressurized sample as a function of time every 20 msec using the Ocean Optics software before and following (at time zero) the actuation of the electronic valve to release the pressure to atmospheric (14.3 psi). Emission intensity data obtained by this method show a very fast initial change followed by a characteristic long tail due to the diffusional nature of the sample equilibration. The integrated emission response at 47.8 psi was subtracted from all of the data points and then the resulting data were normalized so that the integrated emission at infinity (P = 14.3 psi) was 1. The plot of this normalized response vs time is displayed in Figure 3.

Solid-State Photophysical Measurements. Solid-state quantum yields of the compounds were obtained by a modification of the method described by Wrighton et al.[36] A Fluorilon scattering target was used instead of MgO. The methods used to obtain and correct the data for detector response have been described previously.[11] Some representative corrected spectra are shown in the Supporting Information. Solid-state emission lifetimes were obtained with an in-house constructed circuit that pulses an LED for excitation of the sample. The light was conducted through one leg of a bifurcated fiber optic probe to the sample housed in a sample compartment identical to the one used for the Stern−Volmer measurements. The emission decay and scattered light were collected by the other fiber optic leg, filtered through a cut off filter to remove the scattered excitation light and conducted to a Hamamatzu R928 PMT. The PMT signal was digitized by a sampling digital oscilloscope (Phillips PM 3323) interfaced to a computer running a LabView program similar to the one used for control of the Stern−Volmer data collection system. More details concerning the lifetime data acquisition and processing have been presented previously.[11]

Results and Discussion

Molecular Oxygen Sensing. It has previously been demonstrated that copper compounds can be utilized as photoluminescent oxygen sensors when dispersed in a support material.[12,13] As stated in the introduction, our aim was to remove the need for the support material and use these pure, crystalline Cu(I) compounds as oxygen

(36) Wrighton, M. S.; Ginley, D. S.; Morse, D. L. *J. Phys. Chem.* **1974**, *78*, 2229–33.

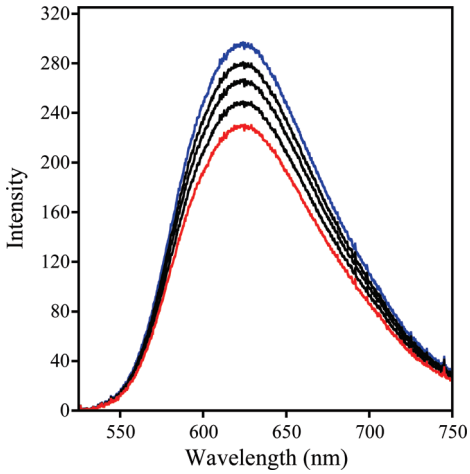

Figure 1. Uncorrected emission spectra excited at 400 nm for [Cu(dipp)$_2$]tfpb (**3b**) under varying amounts of O_2 in N_2. The spectra under pure nitrogen and pure oxygen are shown in blue and red, respectively. Mole fraction of O_2 in N_2 from top to bottom is 0, 0.193, 0.379, 0.659, 1.

sensors. Compounds **1a**−**4b**, selected as good initial candidates for these studies, were synthesized in good yields, crystallized from methanol/water, and found to be pure via NMR and mass spectrometry. Luminescence spectra, excited at 400 nm, of pure crystalline samples of compounds **1a**−**4b** were obtained under pure N_2 and O_2 to screen their viability as oxygen sensors. Spectra collected for several oxygen concentrations are shown for [Cu(dipp)$_2$]tfpb (**3b**) in Figure 1. Among the eight compounds screened, **1a**, **2a**, and **4a** did not show sensing ability above our level of detection (K_{sv} = 0.005); **1b** is a very marginal oxygen sensor and **2b**, **3a**, **3b**, and **4b** are relatively good sensors with [Cu(dmp)(dbp)]tfpb (**4b**) and especially [Cu(dipp)$_2$]tfpb (**3b**) the most sensitive. Figure 2 displays the Stern−Volmer (SV) plots (I_o/I −1 vs mole fraction of oxygen in nitrogen) for samples of **3a**, **4b**, and **3b**. Plots were linear and yielded highly reproducible K_{sv} values of 0.103(4), 0.155(4)and 0.299(7), respectively. These values can be compared with the value (0.56) reported by Karpishin et al. for [Cu(dmp)(dbp)]PF_6 in polystyrene.[12] Somewhat unexpectedly, one of the BF_4^- salts ([Cu(dipp)$_2$]BF_4 (**3a**)) also shows significant sensing ability suggesting that tfpb$^-$ is not absolutely necessary for oxygen sensing. The observation of straight line SV plots for these three compounds is consistent with the presence of a single crystallographic sensing site (vide infra). This is of practical significance because once the Stern−Volmer constant is found for one sample, in principle, sensors can be made to determine the oxygen percentages from any other sample with only one reference value needed (for example, under air). This single point calibration would be useful only for sensor compounds that are very stable and highly reproducible.

The standard deviations of the K_{sv} measurements encompass three determinations each of three different samples prepared and measured in a similar manner over a period of up to 5 days. The values for a given sample were also found to be stable over a period of at least 2 days. A few samples that were stored in air for several

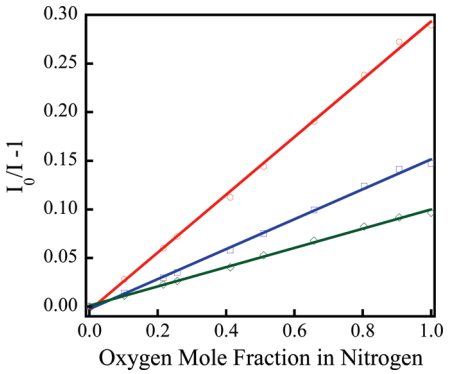

Figure 2. Stern−Volmer plots ($(I_0/I) - 1$ vs mole fraction of oxygen in nitrogen) for typical samples of **3a** (green diamonds), **3b** (red circles), and **4b** (blue squares); the lines are the appropriate linear regression fits. Three cycles were collected over a 15 h period for each sample; one cycle is displayed for clarity.

weeks were remeasured and found to have Stern−Volmer plots virtually identical to those initially measured. Samples of some of the compounds that were stored in laboratory air for up to 2 years gave sensing determinations virtually identical to samples prepared in the immediate past. To confirm that these film measurements result from the crystal structure obtained by single-crystal X-ray crystallography, a single crystal of **3b** was placed into a depression in a Delrin rod and a full concentration range Stern−Volmer experiment was performed. This single crystal experiment yielded a K_{sv} value of 0.3065, which lies almost perfectly in the center of the tight range of values obtained for the thin crystalline films of this compound.

In summary, the quenching of the emission from samples of crystalline **2b**, **3a**, **3b**, and **4b** by gas phase O_2 is significant, reversible and reproducible. The observed response time is approximately 45 s for all of the compounds studied in the sensing apparatus, but the actual response time of the samples is considerably faster. The results of a pressure jump experiment between 47.8 and 14.7 psi for **3b** are shown in Figure 3. The 50% and 95% response times are 77 and 280 ms, which compare favorably to the 50% response time (20 msec) previously reported for [Ru(phen)$_3$](tfpb)$_2$.[11]

Photophysics. It is necessary for viable oxygen sensors of this type to also show good solid-state emission properties in addition to the actual quenching processes. For example, high quantum yields are necessary so that LED excitation and photodiode detection of the emission intensity changes due to oxygen concentration will be possible. The first absolute solid-state quantum yields for $[Cu(NN)_2]^+$ compounds are reported in Table 2. These range from about 0.001 to 0.139, with the two best oxygen sensors ([Cu(dmp)(dbp)]tfpb and [Cu(dipp)$_2$]tfpb) exhibiting significant quantum yields of approximately 0.12 and 0.02, respectively. In both of these cases the emission intensity exhibited by samples excited by the 400 nm LEDs employed in our studies is easily detectable with an inexpensive CCD spectrometer. In general, many of the observed quantum yields reported here are considerably higher than those measured previously for similar

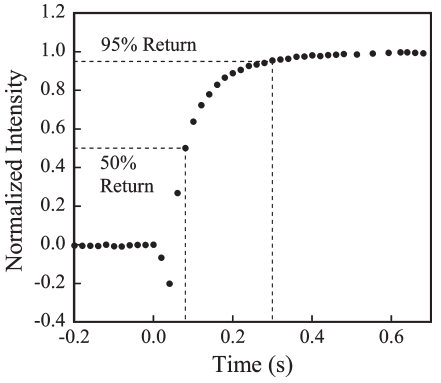

Figure 3. Pressure jump experiment performed on a crystalline film of $[Cu(dipp)_2]tfpb$ cast from MeOH. The cell was pressurized to 47.8 psi and then at $t = 0$, the pressure was released to atmospheric pressure. The times for 95 and 50% return are 0.28(1) and 0.077(6) s, respectively. Excitation was performed with a 400 nm LED.

compounds in solution.[37] For example, comparison of solution-state $[Cu(dmp)(dbp)]^+$ ($\Phi = 0.010$) to solid-state [Cu(dmp)(dbp)]tfpb ($\Phi = 0.12$) displays an approximate 10-fold increase.

The solid-state luminescence lifetimes were determined for compounds **1a**−**4b** as previously described.[11] These range from ~ 250 ns for **2a** all the way up to 3.44 μs for **4b** under nitrogen. The lifetimes under oxygen showed quenching that is reasonably consistent with the more accurately determined emission intensity SV measurements. All of the compounds except **3a** and **4a** exhibit monoexponential decay under both gases. Representative plots of the natural logarithm of the emission intensity as a function of time for $[Cu(dipp)_2]tfpb$ (**3b**) under nitrogen and oxygen are shown in Figure 4. The lifetime data for **3a** and **4a** were fit to biexponential decays; in the case of **3a**, the observed biexponential decay is explained by the disorder of the BF_4^- counterion over two positions in the asymmetric unit to yield two different emitting Cu(I) centers in the crystal. We are unable to comment directly as to the reason of the biexponential decay of compound **4a** because the crystal structure was not determined for lack of suitable crystals. In general, these lifetimes are also significantly increased from the solution state, by approximately the same factor of 10 as the quantum yields.[37−39] A comparison of the radiative and nonradiative rates in solution[38] and the solid state for the same cations ($[Cu(dmp)_2]^+$, $[Cu(dipp)_2]^+$, and $[Cu(dbp)(dmp)]^+$) reveals that the decrease in the nonradiative rate from solution[38] to the solid state is much more significant than the increase in radiative rate. It has been shown that the distortion from tetrahedral to square planar in the MLCT excitation[38,39] in solution and the solids increases the nonradiative decay rates. Some inhibition of this distortion in the crystalline state can explain the observed effect on these radiative and nonradiative rates.

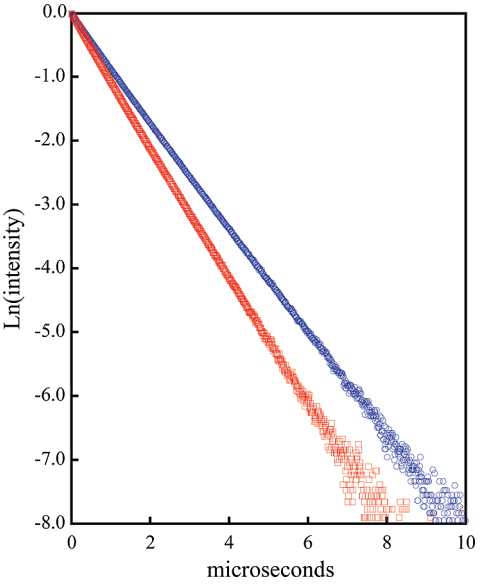

Figure 4. Plots of ln(emission intensity) vs time for crystals of $[Cu(dipp)_2]tfpb$ (**3b**) under nitrogen (blue circles, $\tau = 1.17\ \mu s$) and oxygen (red squares, $\tau = 0.946\ \mu s$).

Diffusion and Quenching in the Crystalline State. The nature of the gas phase quenching of the crystalline samples with oxygen has been previously investigated for $[Ru(phen)_3]^{2+}$ salts.[11] A discussion of this phenomenon is facilitated by reference to eqs 1 and 2, which are the Stern−Volmer relationship (1) and the expansion of K_{sv}' for fixed position emitting sites (2)[40]

$$\frac{I_0}{I} = 1 + K_{sv}' pO_2 \tag{1}$$

$$K_{sv}' = \tau_0 f N_A 4\pi D_{O_2}(r_L + r_{O_2}) S_{O_2} \tag{2}$$

where p_{O_2} is the partial pressure of O_2, τ_0 is the lumophore lifetime, f is a statistical factor, N_A is Avogadro's constant, D_{O_2} is the O_2 diffusion constant, r_L and r_{O_2} are the encounter radii, and S_{O_2} is the solubility of O_2 in the crystal. Previously,[11] we showed that surface quenching by exciton migration is not a factor for materials such as these with well separated cations so an additional term that would allow for diffusion of the excited state to the surface is not included in this equation.

The two terms most important to this discussion are the product $D_{O_2}S_{O_2}$ and τ_0, which represent the permeability[41] of oxygen through the crystalline lattice and the intrinsic lifetime of the excited state, respectively. The net Stern−Volmer quenching observed is directly proportional to both of these factors which are controlled by the crystal structure and the photophysics of the $[Cu(NN)_2]^+$ cation, respectively. As the presence of void space was previously found to be the most important predictor of molecular oxygen sensing ability,[11] the emphasis of our structural data analysis was to characterize the amount and quality of void space in the crystals.

(37) Eggleston, M. K.; McMillin, D. R.; Koenig, K. S.; Pallenberg, A. J. *Inorg. Chem.* **1997**, *36*, 172–176.
(38) Scaltrito, D. V.; Thompson, D. W.; O'Callaghan, J. A.; Meyer, G. J. *Coord. Chem. Rev.* **2000**, *208*, 243–266.
(39) Kovalevsky, A. Y.; Gembicky, M.; Coppens, P. *Inorg. Chem.* **2004**, *43*, 8282–8289.
(40) Frank, R. S.; Merkle, G.; Gauthier, M. *Macromolecules* **1997**, *30*, 5397–5402.
(41) Biscoglio, M. *J. Phys. Chem. B* **1999**, *103*, 9070–9079.

As outlined in the Experimental Section (and more fully discussed in the Supporting Information) the solvent accessible void space (expressed as a fraction of the unit-cell volume) was calculated for each crystal structure (with the exception of compound **4a**, where no structure is available) and is given in Table 2. Our hypothesis is that void space is a necessary but not sufficient condition for oxygen sensing in these compounds. The lack of oxygen sensing for compound **2a** correlates well with the absence of void space suggested by the crystallographic analysis. Compound **4a** is also not an oxygen sensor but the X-ray structure is not available so further discussion of this compound is unwarranted. The sensing behavior of compound **1a** requires additional analysis because it has void space (2.1%) but it is not an oxygen sensor.

In the previously studied $[Ru(phen)_3](tfpb)_2$[11] compound, $[Ru(5,6\text{-dmp})_3](tfpb)_2$[10] and chiral $[Ru(phen)_3](PF_6)_2$,[9] the void space present in each crystal structure was significant and in the form of channels so an obvious pathway for oxygen diffusion is present. Visual examination of the void space depictions for all of the copper complex $tfpb^-$ structures studied here revealed no clear indication of channels and only a partial channel in one of the BF_4^- structures (**3a**) as a consequence of the disorder in the BF_4^- anions (vide infra). As in the case of glassy polymers such as PTMSP (poly(1-trimethylsilyl-1-propyne)) and Teflon AF2400 (a 13:87 copolymer of tetrafluoroethylene and 2,2-bis(trifluoromethyl)-4,5-difluoro-1,3-dioxole), which exhibit high permeability of oxygen[42] in the solid state, the presence of permanent channels is not necessarily required for oxygen solubility or diffusion if significant molecular motion can occur. In this latter regard, we point out that the void spaces in the $tfpb^-$ structures are lined with highly mobile CF_3 groups that produce a nearly fluorous environment,[43,44] which has been shown to readily dissolve oxygen.[43−45]

The relationship between void space and permeability[46,47] has previously been developed for polymer films (eq 3)

$$S_{O_2} D_{O_2} = \beta(v_a - v_0) De^{-B/FFV} \quad (3)$$

where v_0 and v_a are taken as the reciprocal of the density of a calculated "ideal close packed" structure and an experimental structure that might have void space, respectively; the $\beta(v_a - v_0)$ term is the solubility of oxygen in the free space in the solid with $(v_a - v_0)$ as the free volume per gram and β a proportionality factor; the diffusion coefficient of oxygen through the solid is $De^{-B/FFV}$ with D a proportionality factor, FFV the fraction of free volume in the polymer $((v_a - v_0)/v_a)$ and B a constant that characterizes the size of the diffusing species

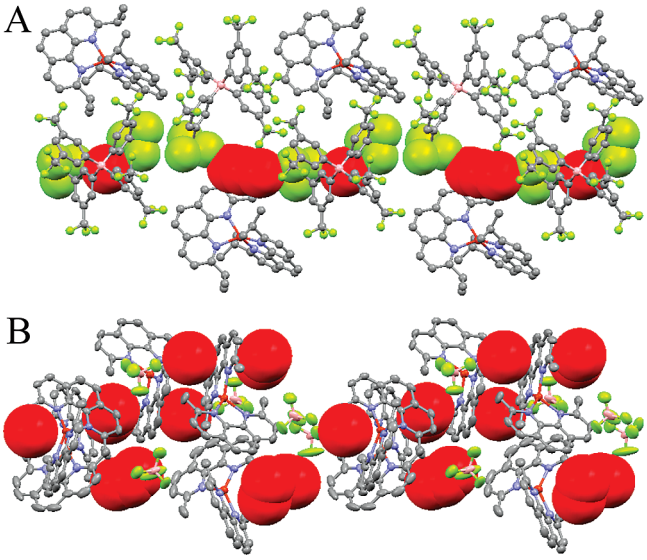

Figure 5. Depictions of the calculated void space as red space filling spheres for compounds (A) **3b** and (B) **1a**. Compound **3b**, a good oxygen sensor, has void space lined with CF_3 groups (fluorine atoms shown as green space-filling spheres), whereas compound **1a** contains isolated void space separated by the cations and does not sense O_2.

relative to the size of an inter void space passage. It is clear that this equation allows for the presence of isolated void space that will not support rapid oxygen diffusion through the solid. To support oxygen molecule diffusion through a channel (as in the case of $[Ru(phen)_3](tfpb)_2$[11]), B either needs to be small or it can become small by a thermally activated process that enables oxygen molecules to move from void to void as in the case of crystalline C_{60}[48−50] or glassy polymers.[51] Close examination of the void space present in the crystal structures of compounds **2b**, **3b**, and **4b**, (all good sensors) show that the void cavities, although not channels, are lined with highly mobile CF_3 groups (illustrated for **3b** in Figure 5A), some of which are still severely disordered even at temperatures as low as 123 K. In the case of compound **1a** (a nonsensor with ordered BF_4^- and voids, but no channels), the cations block the connectivity of the void cavities (Figure 4B); in the case of compound **3a** (another BF_4^- salt, but with positional disordering of the BF_4^-), a continuous channel is present through a unit cell for one of the BF_4^- positions (0.76 occupancy) but not the other (see the Supporting Information for details). In this case, oxygen sensing is observed but at a level somewhat less than expected for the rather high weighted average void space fraction (6.3%) calculated. In summary, we have found that void space is a prerequisite for oxygen sensing ability in these compounds but it is not an absolute requirement that it be present in the form of channels if there are mobile functional groups (i.e., CF_3) that can be easily thermally activated to allow the passage of oxygen molecules from cavity to cavity.

(42) Merkel, T. C.; Bondar, V.; Nagai, K.; Freeman, B. D.; Yampolskii, Y. P. *Macromolecules* **1999**, *32*, 8427–8440.
(43) Gladysz, J. A.; Curran, D. P.; Horvath, I. T. *Handbook of Flurorous Chemistry*; Wiley: New York, 2004.
(44) Hamza, M. H. A.; Serratrice, G.; Stebe, M. J.; Delpuech, J. J. *J. Am. Chem. Soc.* **1981**, *103*, 3733–8.
(45) Hamza, M. H. A.; Serratrice, G.; Stebe, M. J.; Delpuech, J. J. *J. Magn. Reson.* **1981**, *42*, 227–41.
(46) Ronova, I. A.; Rozhkov, E. M.; Alentiev, A. Y.; Yampolskii, Y. P. *Macromol. Theory Simul.* **2003**, *12*, 425–439.
(47) Hu, Y. S.; Liu, R. Y. F.; Zhang, L. Q.; Rogunova, M.; Schiraldi, D. A.; Nazarenko, S.; Hiltner, A.; Baer, E. *Macromolecules* **2002**, *35*, 7326–7337.
(48) Halac, E.; Burgos, E.; Bonadeo, H. *Phys. Rev. B: Condens. Matter* **1995**, *52*, 4764–7.
(49) Gu, M.; Tang, T. B.; Hu, C.; Feng, D. *Phys. Rev. B: Condens. Matter Mater. Phys.* **1998**, *58*, 659–663.
(50) Yang, C.-M.; Liao, J.-L.; Chiu, K.-C. *J. Appl. Phys.* **2004**, *96*, 1934–1938.
(51) Dlubek, G.; Pionteck, J.; Raetzke, K.; Kruse, J.; Faupel, F. *Macromolecules* **2008**, *41*, 6125–6133.

The remaining variation in the observed K_{sv} values we report here can be understood in terms of the excited state lifetime of the crystalline sensor material. Compounds **3b** and **4b** have a similar void space fraction comparable to compound **2b**, but have longer lifetimes, which lead to larger observed K_{sv} values. We suggest that increasing the void space will eventually cause the collapse of the crystal structure to a more compact one, so increasing the lifetime will be the best strategy to obtain more efficient molecular O_2 sensors after a structure motif is constructed with at least enough void space to enable some permeability.

Conclusions

We have shown that crystals of a number of the emissive copper compounds from the set **1a**−**4b** are oxygen sensors, specifically if they contain void space. All of the $tfpb^-$ salts were found to be oxygen sensors, reinforcing the idea that bulky counterions can produce void space and obviate the need for a support material in solid-state photoluminescent oxygen sensors. The first solid-state quantum yields and lifetimes are reported for the $[Cu(NN)_2]X$ ($X = BF_4^-$, $tfpb^-$) systems and are found to be approximately 10 times larger than those observed in solution-state measurements. The linear Stern−Volmer plots with highly reproducible K_{sv} constants observed from sample to sample and day to day reinforce the observations that the sensing materials are crystalline, stable to air and light, and the sensing sites are homogeneous within the crystals.

Acknowledgment. This work was supported by the Center for Analytical Chemistry at the University of Washington and the Initiative for Renewable Energy and the Environment at the University of Minnesota. The authors thank Dr. Victor G. Young Jr. of the University of Minnesota X-ray crystallography laboratory, Dr. Kari A. McGee, and Professor Doyle Britton for assistance with some of the crystal structures.

Supporting Information Available: Crystal structure refinement details, void-space calculations, sample compartment figure, emission decay for **3b**, corrected solid-state spectra for **3b** and **4b**, and void space diagrams for **3a** (PDF). This material is available free of charge via the Internet at http://pubs.acs.org.